Title : will be set by the publisher
Editors : will be set by the publisher
EAS Publications Series, Vol. ?, 2005

RADIATIVE TRANSFER IN SNAPSHOTS OF 3D RADIATIVE HYDRODYNAMIC MODELS OF RED SUPERGIANTS.

A. Chiavassa[1], B. Plez[1], E. Josselin[1] and B. Freytag[2]

Abstract. Red Supergiant (RSG) represent a key-phase in the evolution of massive stars. These stars are characterized by strong mass loss of unknown origin. Observations show strong line profile fluctuations in depth, width and velocity, suggesting giant convective cells which could explain mass loss.
Recently, radiative hydrodynamics (RHD) simulations of these stars show a peculiar convection pattern with giant cells. We performed 3D pure LTE radiative transfer calculations in snapshots of 3D hydrodynamical simulations taking into account the Doppler shifts caused by the convective motions. Computed spectra from RHD models qualitatively reproduce observations.

1 Introduction

Red supergiants (hereafter RSG) constitute a key-phase in the evolution of massive ($10 \leq M_{init} \leq 30 M_\odot$) stars. RSG are characterized by strong mass-loss ($M \sim 10^{-6} M_\odot$ yr^{-1}; Castor 1993) of unknown origin, and play an important role in the chemical evolution of galaxies due to the various nucleosynthetic processes. The mass-loss process of RSG is still poorly known. Pulsationally-driven winds coupled with radiation pressure on dust are probably irrelevant, as RSG are low-amplitude and irregular variables. Alternative theories linked with acoustic or Alfvén wave driven winds (Hartmann & Avrett 1984, Pijpers & Hearn 1989, Cuntz 1997) should perhaps be considered. The idea of giant convective cells in the atmosphere of RSG was suggested for the first time by Schwarzschild (1975). Considering that the pressure scale-height determines the characteristic scale of convection (in agreement with the Mixing Length Theory), and adopting a constant ratio (diameter of a granule)/(depth of a granule) of about three, he estimated that the

[1] GRAAL, cc072, Université Montpellier II, F-34095 Montpellier cedex 05, France
[2] Department for Astronomy and Space Physics at Uppsala University, Box 515, SE 75120 Uppsala, Sweden

DOI: (will be inserted later)

surface of the star could be occupied by at most a dozen cells.
Hydrodynamical modeling of convection in RSGs has therefore lagged behind that of solar type stars due to the necessity to include the whole star in the simulation box. Recently, Freytag et al. (2002) have succeeded in doing such numerical simulations of a typical RSG showing giant convective cells evolving on a timescale of about one month, supersonic velocities and shocks.
We present here our first attempts to compare these simulations to observations in order to check their reliability.

2 The observer's point of view

RSGs are irregular, small-amplitude variables (Fig.1) and they have complex spectra (Fig.2): strong molecular absorption by TiO and other molecules, which leads to blends and to a continuum level poorly defined. Spectral lines are strongly affected by large velocities present in their atmospheres (Fig.3).

We observed a sample of M supergiants from Humphreys (1978) catalog of bright stars with the echelle spectrograph ELODIE, mounted on the 193 cm telescope at the Haute-Provence Observatory. The spectra cover the wavelength range $3906-6811$ Å with a resolution of 42000 and a typical signal to noise ratio of about 50. The first set of observations was obtained in august 1999, and then we made a time series observations with the same instrument in 2003 and 2004.
We applied to these spectra the tomographic method developed by Alvarez et al. (2001). The spectra are correlated with a set of numerical masks which probe layers at different atmospheric heights, from the innermost (mask C1, containing high excitation lines) to the outermost layers (mask C8, low excitation and resonance lines). This technique takes advantage of the ability of the cross-correlation function (CCF) to reveal complex profiles despite the severe crowding of the optical spectra. The resulting CCF present a wide variety of shapes, depending on the mask and on the star.

Figure 3 shows that weaker lines generally appear blueshifted relative to stronger lines. The correlation profiles (and thus the line profiles) display a strong asymmetry with, in some cases, two or more components. The velocity shifts, between the weak and the strong lines, are up to 25km/s. The peaks of CCF, which shift to red, indicate downward motions of the outer or cooler layers.
Figure 4 shows CCF profiles for α Ori fluctuating in depth, width and velocity, although they are more symmetric and less variable than those of SW Cep. Time-variable structure in line profiles is a natural and necessary consequence of giant convective cells.
Gray (2001) made spectroscopic observations of α Ori and argued that there is no evidence for giant convective cells, since line profiles do not evolve with time. However these observations are not wavelength calibrated on an absolute scale and the lines chosen belong to our mask C5 which is, indeed, not affected by strong variations compared to mask C1 (Fig.4).

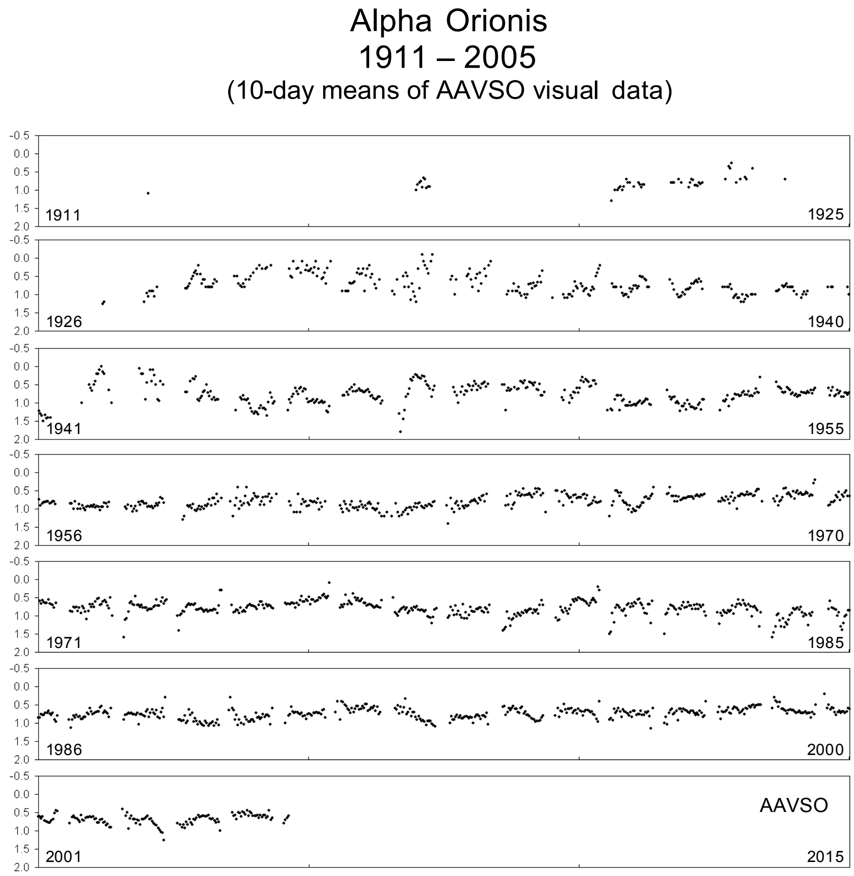

Fig. 1. Typical light curve of a RSG (α Ori) which shows irregular variations of small amplitude. This data is published by permission of the American Association of Variable Star Observers.

3 The modeler's point of view

3.1 1D Modeling

Observations of line profiles help constrain and validate models of RSGs atmospheres. A first approach to reproduce observations has been carried out with 1D hydrostatic models, which fit very well K giant stars (Fig.5). They do not reproduce RSG spectra, as can be seen on Fig.5. Weak and strong lines cannot be fitted with the same model and abundances. In addition, the macroturbulent broadening seems exponential, suggesting a non gaussian distribution of large scale velocities(Josselin & Plez, 2003).

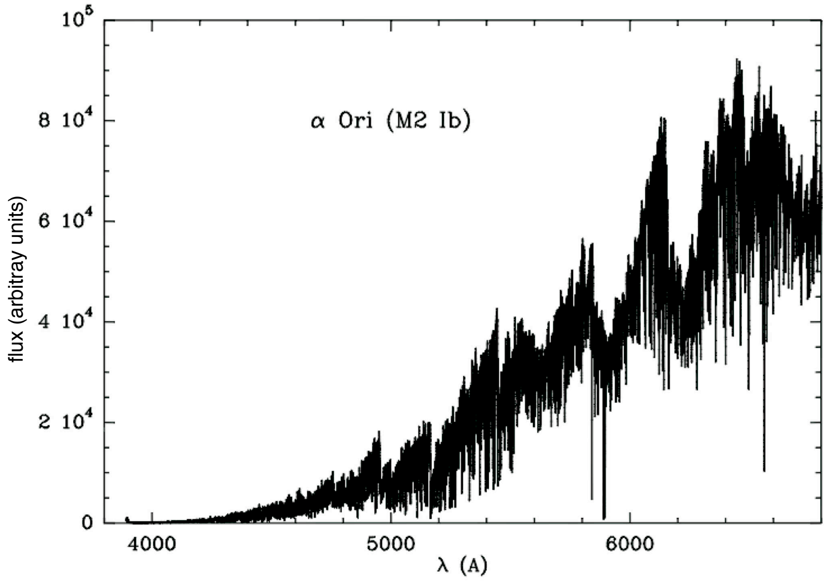

Fig. 2. Optical spectrum of α Ori obtained with the echelle spectrograph ELODIE, mounted on the 193cm telescope at the Haute-Provence Observatory. Note the large number of spectral lines especially of TiO giving rise to large absorption bands. The continuum is poorly defined.

Our purpose is to investigate whether 3D hydrodynamical models, now available, can solve the problems outlined above.

3.2 Modeling with CO^{5}BOLD

The numerical simulations analyzed here are performed with "CO5BOLD" ("COnservative COde for the COmputation of COmpressible COnvection in a BOx of L Dimensions, l=2,3") developed by Freytag, Steffen, Ludwig and collaborators (see Freytag et al., 2002) The RSG simulations presented employ the *global star-in-a-box* setup: the computational domain is a cube, and the grid is equidistant in all directions. Radiation transport is strictly LTE. The grey Rosseland mean opacity is a function of pressure and temperature. The necessary values are found by interpolation in a 2D table which has been merged at around 12 000 K from high-temperature OPAL data (Iglesias et al. 1992) and low-temperature PHOENIX data (Hauschildt et al. 1997) by Hans-Günter Ludwig.
Some more technical informations can be found in the CO5BOLD Online User

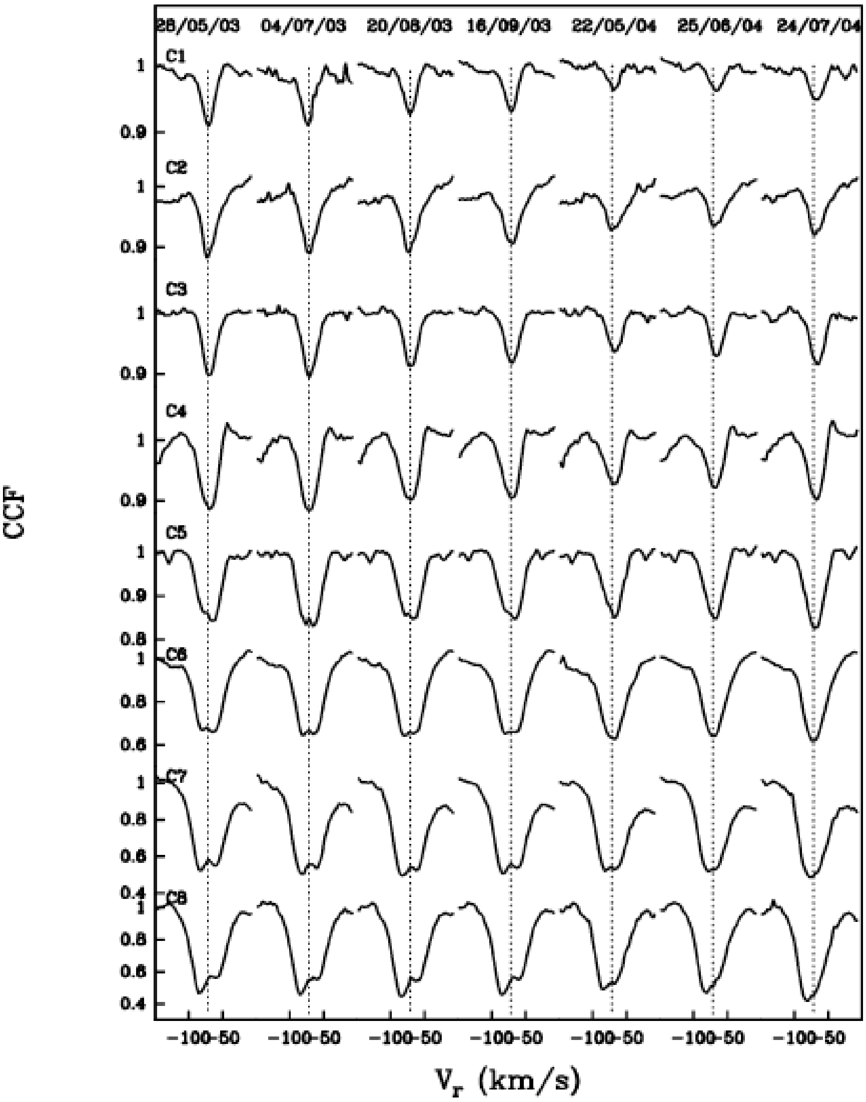

Fig. 3. Tomographic technique developed by Alvarez et al. (2001) (see text) : the image shows cross-correlation functions (CCF) for SW Cep. Each column represents one observation. The correlation profiles display a strong asymmetry with, in some cases, two or more components. The velocity shifts, between the weak and the strong lines, are up to 25km/s.

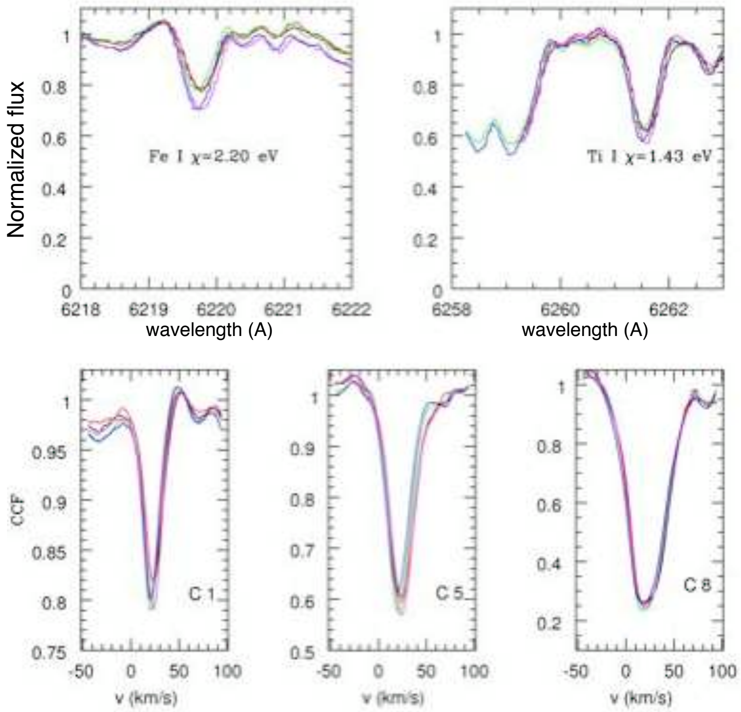

Fig. 4. Spectra and CCF of α Ori : colors correspond to different observation's epoch. The upper panels show a small range of spectra containing two lines observed also by Gray (2001). The lower panels shows CCF for some masks. All the profiles fluctuate in depth, width and velocity, a signature of giant convection cells.

Manual (Freytag et al. 2003).

3.3 Model setup and parameters

The parameters of the "best" RHD model, that has been obtained so far have a solar composition, a resolution of 171^3 grid points, a mass $= 5M_{\odot}$, a stellar luminosity $= 41358L_{\odot}$, an effective temperature of 3210K, $\log g = -0.50$, and a stellar radius $= 657R_{\odot}$.

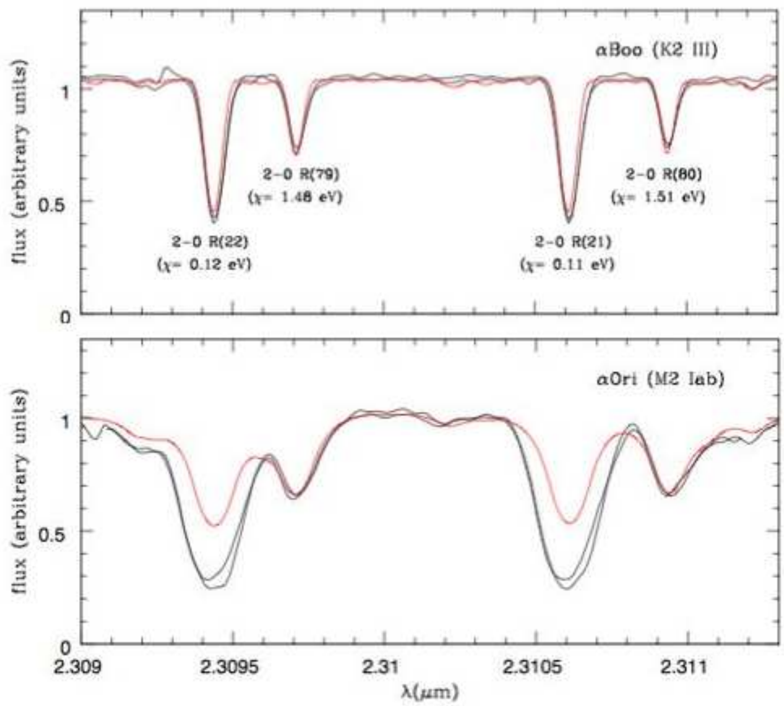

Fig. 5. First approach to reproduce RSG spectra with 1D hydrostatic models around $2.3\mu m$ (CO lines) : upper panel shows that a 1D model spectrum (red line) fits very well a K giant spectrum (α Boo, Wallace & Hinkle, 1996; black line), while in lower panel there is no way to adjust the observation (α Ori spectrum) with a single model (Josselin & Plez, 2003).

3.4 Basic proprieties of the numerical models

Simulations unveil few large envelope convective cells (as predicted by Schwarzschild, 1975), evolving on a timescale of about one month, with supersonic velocities resulting into high-amplitude shock waves. More details will be provided elsewhere (Freytag et al., in preparation).

4 The virtual observer's point of view

Our aim is to compare the 3D hydrodynamical models with observations in terms of line profiles and asymmetries in order to check the reliability of the simulations.

4.1 Post-Processing and method analysis

We performed 3D pure LTE radiative transfer calculations in snapshots of the 3D hydrodynamical simulation, described above, taking into account the Doppler shifts caused by the convective motions. The geometry is shown in Fig.6. The intensity, $I_{\lambda_{ij}}$, emerging on the top of a ray i,j is computed by summing, along the k direction, the contributions of the source function

$$I_{\lambda_{ij}} = \sum_k B_\lambda \left(T_{ijk}\right) \cdot exp\left(-\tau_{\lambda ijk}\right) \delta\tau_{\lambda_{ijk}}. \quad (4.1)$$

The optical depth is computed along the k direction following

$$\tau_{\lambda ijk} = \sum_1^k \chi_{ijk}\left(T_{ijk}, \rho_{ijk}, \lambda \cdot \left(1 - v_{ijk}/c\right)\right) \rho_{ijk} \delta z_{ijk}, \quad (4.2)$$

where χ_{ijk} is the extinction coefficient per mass unit, including all absorption and scattering, shifted with the proper radial velocity v_{ijk}, δz_{ijk} is the thickness of the k cell.
To reduce the computing time, the extinction coefficient is pre-tabulated as a function of T,ρ and λ at a resolution of 0.01 Å. We found that sufficient to ensure an accurate description of line profiles even after interpolation at the Doppler shifted wavelengths.

Pure LTE is assumed and the source function is taken as $S_\lambda = B_\lambda\left(T_{ijk}\right)$, the Planck function at the temperature T_{ijk}.

4.2 First results

Figure 7 shows a time sequence (with a step of about four months, covering 5.7 stellar years) of spectra computed from the model described above. The variations are strong compared to observations (Fig.4). Several causes may generate these fluctuations : (1) model mass is too small, (2) effective temperature is too low, (3) the grey treatment of opacity in RHD models is not appropriate, (4) resolution of RHD models must be improved.

Afterwards we applied again the tomographic technique (Alvarez et al., 2001) to a synthetic spectrum, calculated over a part (3800−4800Å) of the Elodie region, to obtain a cross-correlation function. As the computation of the whole spectral range, before cross correlation with the masks, is rather tedious, we carefully studied the content of each mask in terms of line excitation and oscillator strength. We then defined a set of 8 artificial lines that should reproduce the behavior of the 8 masks. In this context, it will be much easier to understand the dynamics of the line forming region. The result of a trial calculation is reported on Fig.8, that shows the 8 CCFs calculated for a synthetic spectrum and for the set of 8 artificial lines representative of the masks. Looking at the mask CCF, one may notice that there is an asymmetric structure of the peak (i.e. the signature of atmospheric shocks). However, the CCFs for masks C7 and C8 are much narrower than observations

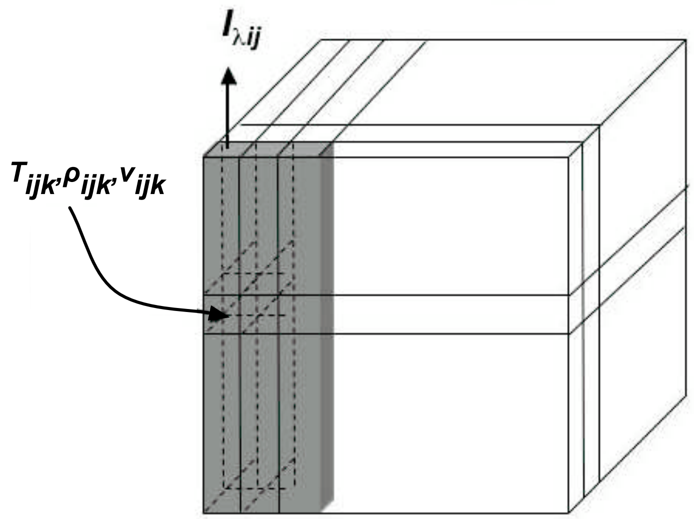

Fig. 6. Geometry of the star-in-a-box model. Temperature, density, velocity are defined in each cube. The emerging intensity is computed by summing contributions over the k direction of the source function (see text).

(Fig.4) and we are currently checking the contribution functions to understand this problem. The 8 artificial line profiles display strong asymmetries with two or more components. Although these asymmetries qualitatively reproduce observations (Fig.4), lines appear much too strong compared to observations. This is due to the lack, in our calculation, of veiling opacity by numerous molecular lines, especially TiO, that strongly reduce the local continuum. We plan to include a pseudo continuous absorption to mimic the veiling.

A last example of what our post-processing code can provide is time and spatially resolved monochromatic intensity maps (Fig.9). We will confront these maps with optical interferometer observations in the near future.

5 Conclusion and perspectives

We are currently working on new models with increased mass and resolution, with parameters closer to prototypical RSG. Table 1, gives the luminosity, the effective temperature, the radius and the gravity of some of our more recent hydrodynamical models. These quantities are averaged over spherical shells and over time. A preliminary analysis of flux fluctuations, in continuum and lines, indicates that these variations diminish with increasing numerical resolution. For a model with 171^3 grid points the fluctuations (calculated for 15 snapshots covering 5.7 years)

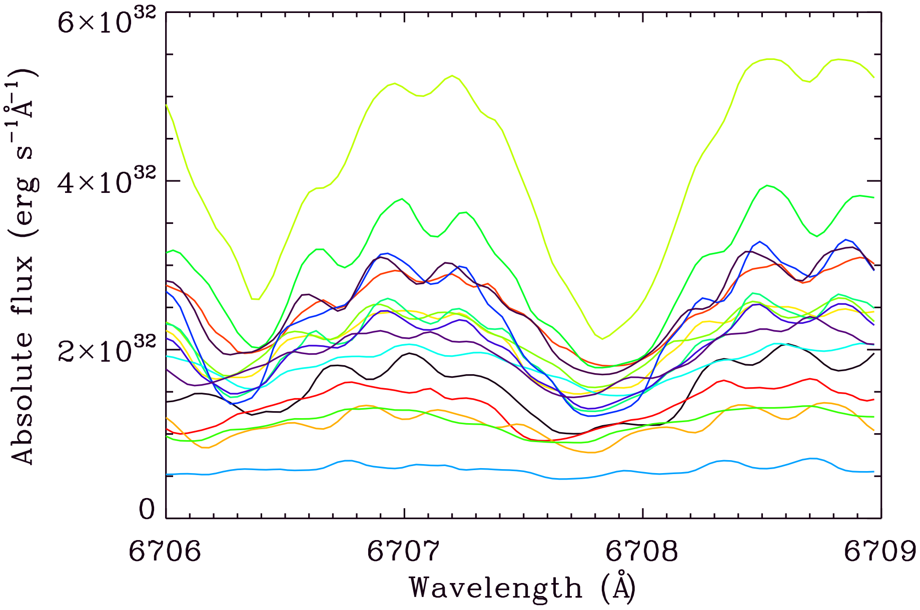

Fig. 7. Flux variations of the spectra computed from the 3210K, $5M_{\odot}$, 171^3 grid points hydrodynamical model analyzed. Each color belongs to a different snapshot with a step of about four months (black is the first time-step and then red to violet), covering 5.7 stellar years. Variations appear strong in comparison with the observations (see Fig.4).

Model	Period coverd (years)	Luminosity ($L_{\odot}$)	$T_{\rm eff}$ (K)	Radius ($R_{\odot}$)	log g	Fluctuations (%) absolute|continuum flux
3210K, $5M_{\odot}$, 171^3	5.7	41358	3210	657	−0.50	±35 | ±20
3297K, $5M_{\odot}$, 315^3	2.5	40000	3297	613	−0.44	±19 | ±11
3382K, $12M_{\odot}$, 315^3	1.3	86701	3382	857	−0.37	±17 | ±10

Table 1. Our most recent models. The stellar parameters are averaged quantities over concentric spheres and over time. We have calculated flux fluctuations. Variations decrease with increasing numerical resolution and, seem also to decrease with increasing temperature around 6700Å.

around an averaged value of absolute flux are about 35%. Doubling the resolution, they drop to about 19% (calculation done for 15 snapshots covering 2.5 years). It is thus necessary to increase the resolution to up to 500^3 grid points, to check if fluctuations will further decrease.

Figure 10 shows the convective structures in different models. Higher grid resolution (315^3 points) models show smaller scale structures, within the larger scale granules that already appear in lower resolution simulations (171^3 points). The

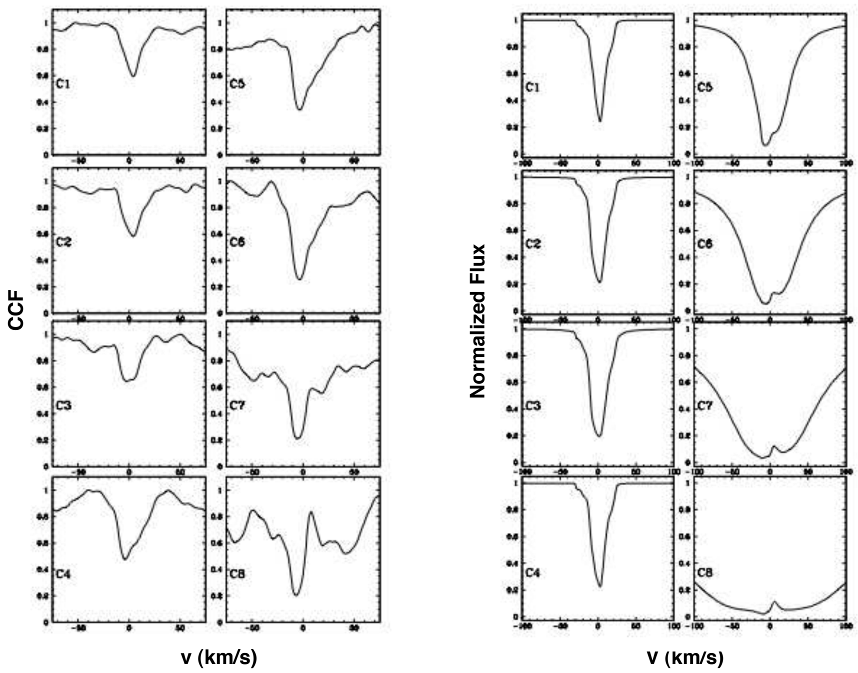

Fig. 8. Results of a first trial calculation with tomographic technique (Alvarez et al, 2001). Left panel shows CCF for a synthetic spectrum calculated over a part of the optical spectrum: an asymmetric structure of the peak is visible (i.e. signature of atmospheric shocks) but some masks show a huge noise which is difficult to remove, we are currently checking the contribution functions to understand this problem. Right panel reports the set of 8 artificial lines: this analysis will let us understand the dynamics of line forming region. However the lack of opacity in the computation shades the reality (for instance masks C6 to C8 should show only the top of the line since the rest is enveloped by a huge TiO band). These results can be qualitatively compared with the CCF profile shapes in Fig.3, considering that this particular analysis refers to a single time-step of stellar evolution model.

size of the structures, the amplitude of fluctuations and the granulation time-scale must be explored more deeply.

Another point of concern is the grey treatment of the radiation field in the hydrodynamical simulations. We are now implementing non-grey opacities, in order to carry out calculations with opacity bins. This is however extremely costly and the number of bins will have to be kept small. This should nevertheless greatly improve the simulations in the atmospheric optically thin layers.

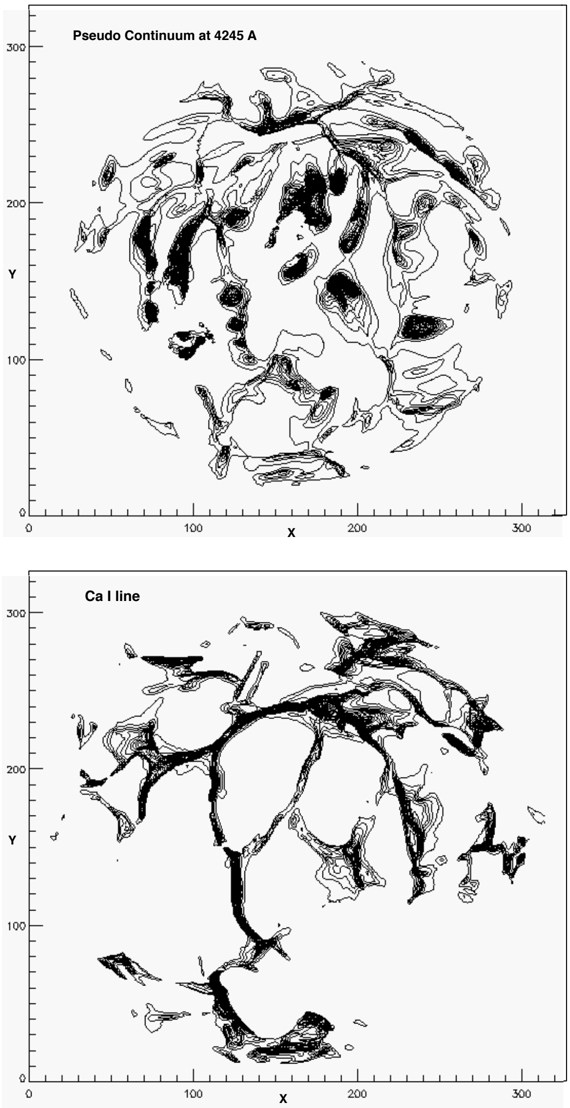

Fig. 9. Example of a spatially resolved continuum (upper panel) and CaI line (lower panel) intensity maps (hydrodynamical model at 3382K, $12M_{\odot}$, 315^3 grid points). We will confront these maps with observations in the near future.

References

Alvarez, R., Jorissen, A., Plez, B., Gillet, D., Fokin, A., & Dedecker, M. 2001, A&A, 379, 288

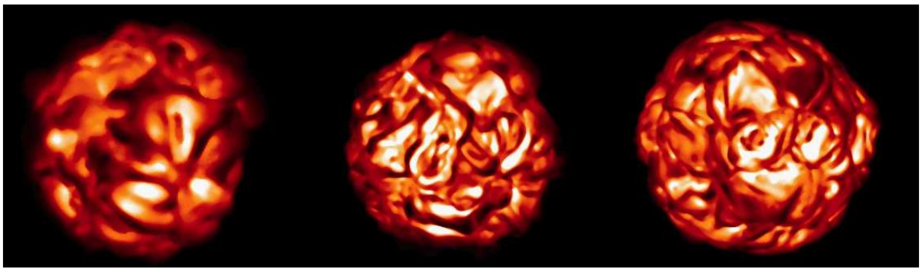

Fig. 10. Convective structures in different models : on the left the $5M_{\odot}$, 3210K, 171^3 grid points model, in the middle the $5M_{\odot}$, 3297K, 315^3 grid points model and on the right the left the $12M_{\odot}$, 3382K, 315^3 grid points model. Higher grid resolution models show smaller scale structures, within the larger scale granules that already appear in the lower resolution simulations.

Castor, J. I. 1993, ASP Conf. Ser. 35: Massive Stars: Their Lives in the Interstellar Medium, 35, 297

Cuntz, M. 1997, A&A, 325, 709

Freytag, B., Steffen, M., & Dorch, B. 2002, Astronomische Nachrichten, 323, 213

Freytag, B., Steffen, M., Wedemeyer, S., & Ludwig, H.-G. 2003, CO5BOLD User Manual

Gray, D. F. 2001, PASP, 113, 1378

Hartmann, L., & Avrett, E. H. 1984, ApJ, 284, 238

Hauschildt, P. H., Baron, E., & Allard, F. 1997, ApJ, 483, 390

Humphreys, R. M. 1978, ApJS, 38, 309

Iglesias, C. A., Rogers, F. J., & Wilson, B. G. 1992, ApJ, 397, 717

Josselin, E., Plez, B. 2003, in High resolution infrared spectroscopy in astronomy, ESO Astrophysics Symposia, eds. H. U. Käufl, R. Siebenmorgen, A. F. M. Moorwood, p.405

Pijpers, F. P., & Hearn, A. G. 1989, A&A, 209, 198

Schwarzschild, M. 1975, ApJ, 195, 137

Wallace, L., & Hinkle, K. 1996, ApJS, 107, 312